A multidimensional analytical approach based on UHPLC-UV-ion mobility-MS for the screening of natural pigments

Journal:	*Analytical Chemistry*
Manuscript ID:	Draft
Manuscript Type:	Technical Note
Date Submitted by the Author:	n/a
Complete List of Authors:	Pacini, Tommaso; University of Iceland, Center For Systems Biology Fu, Weiqi; University of Iceland, Center For Systems Biology Gudmundsson, Steinn; University of Iceland, Center For Systems Biology Chiaravalle, Antonio; Istituto Zooprofilattico Sperimentale di Puglia e Basilicata, Chemistry Brynjolfson, Sigurdur; University of Iceland, Center For Systems Biology Palsson, Bernhard; University of California at San Diego, Bioengineering Department; Univeristy of Iceland, Center For Systems Biology Astarita, Giuseppe; Waters Corporation, ; Georgetown University, Department of Biochemistry and Molecular & Cellular Biology Paglia, Giuseppe; Istituto Zooprofilattico Sperimentale di Puglia e Basilicata, Chemistry; University of Iceland, Center For Systems Biology

A multidimensional analytical approach based on UHPLC-UV-ion mobility-MS for the screening of natural pigments

Tommaso Pacini[1], Weiqi Fu[1], Steinn Gudmundsson[1], A Eugenio Chiaravalle[2], Sigurdur Brynjolfson[1], Bernhard O Palsson[1,3] Giuseppe Astarita[4,5], Giuseppe Paglia[1,2]

1) Center For Systems Biology, University of Iceland, Reykjavik, Iceland;

2) Istituto Zooprofilattico Sperimentale della Puglia e Della Basilicata, Foggia, Italy.

3) Department of Bioengineering, University of California San Diego, La Jolla, CA, USA

4) Department of Biochemistry and Molecular & Cellular Biology, Georgetown University, Washington, DC, USA;

5) Waters Corporation, Milford, MA, USA;

Corresponding Author: Giuseppe Paglia. beppepaglia@gmail.com

Abstract

The online combination of orthogonal analytical tools may improve current methodologies for the analysis of small molecules. Here, we propose a novel strategy that combines a typical ultra high performance liquid chromatography (UHPLC), data-independent mass spectrometry (MS^E) workflow with travelling wave ion mobility (TWIM) and UV detection to improve the characterization of carotenoids and chlorophylls in complex biological matrices. UV detection selectively highlighted pigments absorbing at specific wavelengths, while TWIM coupled to MS was used to maximize the peak capacity. We applied this approach for the analysis of pigments in different microalgae samples, including *Chlorella vulgaris*, *Dunaliella salina* and *Phaeodactylum tricornutum*. Using UHPLC-UV-MS^E information (retention time, absorbance at 450 nm and accurate masses of precursors and product ions), we tentatively identified 26 different pigments (carotenes, chlorophylls and xanthophylls). By adding TWIM information (collision cross sections), we further resolved 5 isobaric pigments, not resolved by UHPLC-UV-MS^E alone. The characterization of the molecular phenotypes allowed us to differentiate the microalgae species. Our results demonstrate that a combination of TWIM and UV detection with traditional analytical approaches increases the selectivity and specificity of analysis, providing a new tool to characterize pigments in biological samples. We anticipate that such an analytical approach will be extended to other lipidomics and metabolomics applications.

Introduction

Carotenoids and chlorophylls are natural pigments synthesized in plants and algae[1]. In these organisms, such pigments synergistically play an essential role in photosynthesis by absorbing light energy and protecting against oxidative damage[2, 3]. In humans, carotenoids are absorbed through diet to become key constituents of skin and eyes. Some of them also serve as precursors of vitamin A[4]. Both carotenoids and chlorophylls present a large number of isomeric species, which makes their chemical identification challenging using traditional analytical approaches.

Carotenoids are prenol lipids that belong to the chemical class of isoprenoids. They are estimated to contain over 600 species, which can be divided into two main groups based on their chemical structures: xanthophylls and carotenes. Xanthopylls contain oxygen such as hydroxy, epoxy, keto, metoxy or carboxylic groups. Carotenes are instead purely hydrocarbons, and contain no oxygen.

Chlorophylls are a family of pigments characterized by a chlorin ring that can be linked to various side chains, most often a phytol chain. Among the various forms of chlorophylls, chlorophyll a and chlorophyll b are the most widely distributed in plants and algae.

Historically, liquid chromatography (LC) in combination with spectrophotometry or mass spectrometry (MS) detection has been used to analyze such natural pigments[5-18]. Recently, we proposed an ultra high performance liquid chromatography (UHPLC)-UV-data independent (MS^E) approach to simultaneously collect both unfragmented and fragmented ions for high-throughput quantitative and qualitative applications[19]. It

is generally accepted, however, that a single analytical technique might be not sufficient to screen the entire natural pigment composition in biological samples and, therefore, multiple technologies are needed for a comprehensive analysis[20].

The combination of travelling wave ion mobility (TWIM) with MS[21-23] is gaining popularity in the field of plant metabolomics[24-26]. Such an approach has been succesfull employed to increase peak capacity[27-29], improve structural elucidation[30, 31] and separate isomeric species[31, 32]. In TWIM-MS, ions are separated in the gas phase according to their charge, shape and size before reaching the mass spectrometer detector. From the time an ion takes to pass through an ion mobility separation cell, it is possible to derive its rotationally-averaged collision cross section (CCS), which provides an orthogonal physicochemical measurement in addition to the mass value for its identification[21, 23, 33-35]. We hypothesized that a combination of TWIM-MS with a spectrophotometric detection can add further selectivity and specificity to the analysis of pigments.

In this study, we combined UHPLC-TWIM-MS^E with spectrophotometry adding a new level of orthogonality to the analysis during a single acquisition. We demonstrated the wide applicability of this approach by phenotyping the pigment content of various microalgae samples.

Experimental Section

Chemicals

All materials were obtained from Sigma-Aldrich (Seelze, Germany) unless stated otherwise. All chemicals and solvents were of analytical grade or higher purity. Acetonitrile was purchased from Merck (Darmstadt, Germany). Water was obtained using an 18 Ωm Milli-Q (Millipore, USA). Lutein, β-carotene, chlorophyll a and chlorophyll b were purchased from Sigma-Aldrich (Seelze, Germany).

Microalgal Cultures

All the species of microalgae were cultivated in bubble column photobioreactors (PBRs) that were equipped with light-emitting diodes (LEDs) and had working volumes of 300 ± 5 ml (PBR dimensions: diameter, ~4 cm; height, ~30 cm), utilizing 1.0%-2.5% CO_2 concentrations in air at 25 ± 3 °C. For cultivation of *Chlorella vulgaris* (UTEX 26, UTEX Culture Collection of Algae), K-8 medium was used and red LEDs with a photon flux of 255 μE/m^2/s were provided as described in our previous studies [36, 37]. *Dunaliella salina* (UTEX LB #200) and the diatom *Phaeodactylum tricornutum* (CCAP 1055/1) were cultured on Gg-8 medium and modified f/2+Si medium (Guillard's medium for diatoms), respectively. Combined red and blue LEDs with a photon flux of 204 μE/m^2/s were used for both *D. salina* and *P. tricornutum*.

Sample Preparation

All microalgae samples were processed by centrifuging 0.5 ml aliquot of cell suspension at 1000×g for 10 min. Next, the cell pellet was extracted using 3 ml of

ethanol:hexane 2:1 (v/v) containing 0.1% (w/v) butylated hydroxytoluene[13, 38]. Further 6 mL of water:hexane 1:2 (v/v) were added and the mixture was vigorously shaken and centrifuged again at 1000 × g for 5 min. The hexane layer was collected (4 ml) and dried, reconstituted in methyl tertiary butyl ether:acetonitrile (MTBE:ACN) (50:50) and 5 µL were injected in the UHPLC system.

UHPLC-UV-TWIM-MS^E Settings

UHPLC separation was performed on an ACQUITY UPLC (Waters, Milford, USA) using a HSS T3 1.8µm (2.1 x 150 mm) column as previously described [39]. A TUV detector (Waters, Milford, USA) was used for on-line UV detection at 450 nm. The UHPLC-UV system was coupled in line with a Synapt G2 (Waters, Wilmslow, UK) operating in positive mode. The capillary and cone voltage were 1.5 kV and 30 V, respectively. The source and desolvation temperature were 100 °C and 500°C, respectively, and the desolvation gas flow was 800 L/hr. Leucine enkephalin (2 ng/µL) was used as lock mass (*m/z* 556.2771). Nitrogen, the ion mobility gas, flowed at a rate of 90 mL/min (3.2 mbar), with a wave velocity of 650 m/s and wave height of 40 V. The EDC delay coefficient was specified as 1.58 V. Data were acquired in HDMS^E mode from *m/z* 50 to 1000, creating two discrete and independent interleaved acquisition functions. Argon served as collision gas and the collision energy in the trap cell was 4 eV (Function 1), and in the transfer cell, it ranged from 30 eV to 40 eV (Function 2).

Collision Cross-Section

CCS values for pigments were determined using the approach previously described [21, 23]. Poly-DL-alanine was prepared in H_2O:ACN (50:50, v:v) at a concentration of 10

mg/L and was used as calibrant using previously published CCS values for singly charged polyalanine oligomers in nitrogen [34, 35]. Calibration was performed using oligomers from n = 3 to n = 11, covering a mass range from 231 Da to 799 Da and a CCS range from 151 $Å^2$ to 306 $Å^2$ in ES+ and from 150 $Å^2$ to 308 $Å^2$ in ES- [34]. CCSs were derived using a procedure previously reported[34]. The ion mobility resolution was ~40 (FWHM).

Data Processing and Analysis

Progenesis QI (Nonlinear Dynamics, Newcastle, UK) was used for processing multi-dimensional UHPLC-TWIM-MS^E data. Isotope and adduct deconvolution was applied to reduce the number of features detected. Data was normalized using total ion intensity. The software was coded to directly convert drift time data into CCS values using the polyalanine calibration curve. TargetLynx was used for processing UHPLC-UV data.

An in house-made algorithm for MATLAB (Electronic Supporting Info) was used for aligning UHPLC-UV and UHPLC-TWIM-MS retention times using a time tolerance of 0.08 min.

METLIN [40, 41] and LIPID MAPS[42] were used as databases. Principal Component Analysis (PCA) and Hierarchical Clustering Analysis (HCA) were performed by using MetaboAnalyst[43]. Before PCA, data was normalized by the sum, log transformed and then scaled by transform to mean zero and unit standard deviation. HCA was obtained by applying the Spearman's rank correlation, while the clustering algorithm used was the Ward's linkage.

Results and Discussion

A typical metabolic profiling experiment provides thousand of ion features representative of a wide range of chemical structures present in a biological sample. This large amount of information makes the identification of metabolites extremely time-consuming[44]. In this work, we show that a combination of UHPLC-TWIM-MS^E [21, 23] and spectrophotometric detection provides a rapid characterization and identification of pigments, such as carotenoids and chlorophylls, in complex biological matrices. We applied this approach for phenotyping the pigment content of various microalgae species.

Selective Pigments Identification

The UHPLC-UV-TWIM-MS^E analysis of the three different microalgae samples investigated provided the detection of 6952 ion features. Each of them was characterized by specific retention time (RT), *m/z,* CCS values and absorbance information [21, 23, 39, 45].

To highlight pigments, we used absorbance information as filter (Figure 1), resulting in the selective extraction of ion features absorbing at 450 nm. We achieved this objective by aligning absorbance and TWIM-MS information according to their chromatographic retention times (Figure 1). Such an approach reduced the number of features of almost four times (from 6952 to 1828), and allowed us to focus our effort on the identification of those features that are representative of the pigments content in algae samples (Figure 1).

To identify the pigments, we searched accurate mass measurements, fragmentation information and retention times against on-line and in-house databases [40, 42].

The addition of TWIM resulted in a 15% increase in peak capacity compared to traditional UHPLC-UV-MS^E analysis (Figure 2). In fact, of the 31 pigments identified, 5 co-eluting isobaric carotenoids were resolved only using ion mobility (Figure 2, Table 1).

Moreover, ion mobility coupled with data-independent acquisition mode (TWIM-MS^E) provided reliable fragmentation spectral data. For instance, the feature identified as fucoxanthin at *m/z* 659 and RT 6.36 min, was further separated into three ion mobility peaks with specific CCS values (Table 1). Characteristic product ion spectra for each of these resolved peaks at *m/z* 659 suggested the existence of isomeric species (Figure 3).

These results show that adding TWIM as an orthogonal dimension increases the specificity and selectivity of the analysis over traditional MS approaches, improving the identification confidence [27, 46-48].

Phenotypic Differentiation of Microalgal Species

This novel UHPLC-UV-TWIM-MS^E approach was applied for the analysis of pigments extracted from three different microalgae: *C. vulgaris*, *D. salina* and *P. tricornutum*. The green algae *C. vulgaris* and *D. salina* belong to the phylum Chlorophyta, and the diatom *P. tricornutum* is in the phylum Heterokontophyta[49]. Their phylogenetic diversity results in unique metabolic pathways[49] and, consequently, it might lead to a different pigment profile.

To test this hypothesis, we setup our UHPLC-UV-TWIM-MS^E approach to compare these three microalgae species. The pigment content of the different algal species clustered into three regions according to their pigment content, as shown by PCA (Figure 4a). The first principal component (PC1) accounts for 52% of the total variance, and mainly separates the microalgae according to the phylum they belong (Figure 4a). The separation of *C. vulgaris* and *D. salina*, which belong to the same phylum, is less pronounced and occurs in the second principal component (PC2) (Figure 4a).

We identified specific pigments that are characteristic of their phylogenetic origins (Figure 4b). While fucoxanthin and diadinoxanthin isomers were only detected in the *P. tricornutum,* chlorophyll b metabolites were only detected in the green algae *C. vulgaris* and *D. salina.* Such results demonstrate that the proposed UHPLC-UV-TWIM-MS^E approach is suitable for the phenotypic characterization of the pigment composition in microalgae.

Conclusion

In this study, we developed an UHPLC-UV-TWIM-MS^E method for the analysis of pigments in plants, which provides five levels of information in a single acquisition: retention time, CCS, absorbance, accurate mass measurements for precursor ions and fragments. The method was applied to the analyses of pigments extracted from various microalgae allowing to increase the overall peak capacity and consequently to improve the characterization of pigments. Using the 31 pigments identified, including we were able to differentiate the three microalgae extracts based on their pigments content.

We anticipate that such an UHPLC-UV-TWIM-MS^E analytical strategy can be extended to the analysis of pigments in other biological systems, facilitating their characterization.

Acknowledgments

The Icelandic Technology Development Fund supported this research.

Supporting Information Available

Matlab code used for aligning UV and TWIM-MS retention times.

References

(1) Walter, M. H.; Strack, D. *Nat Prod Rep* **2011**, *28*, 663-692.

(2) Matthews, P. D.; Luo, R.; Wurtzel, E. T. *J Exp Bot* **2003**, *54*, 2215-2230.

(3) Polivka, T.; Frank, H. A. *Acc Chem Res* **2010**, *43*, 1125-1134.

(4) Fraser, P. D.; Bramley, P. M. *Prog Lipid Res* **2004**, *43*, 228-265.

(5) Bino, R. J.; Ric de Vos, C. H.; Lieberman, M.; Hall, R. D.; Bovy, A.; Jonker, H. H.; Tikunov, Y.; Lommen, A.; Moco, S.; Levin, I. *New Phytol* **2005**, *166*, 427-438.

(6) Moco, S.; Capanoglu, E.; Tikunov, Y.; Bino, R. J.; Boyacioglu, D.; Hall, R. D.; Vervoort, J.; De Vos, R. C. *J Exp Bot* **2007**, *58*, 4131-4146.

(7) Ben-Amotz, A.; Lers, A.; Avron, M. *Plant Physiol* **1988**, *86*, 1286-1291.

(8) Pott, I.; Marx, M.; Neidhart, S.; Muhlbauer, W.; Carle, R. *J Agric Food Chem* **2003**, *51*, 4527-4531.

(9) Ranga Rao, A.; Raghunath Reddy, R. L.; Baskaran, V.; Sarada, R.; Ravishankar, G. A. *J Agric Food Chem* **2010**, *58*, 8553-8559.

(10) Ranga, R.; Sarada, A. R.; Baskaran, V.; Ravishankar, G. A. *J Microbiol Biotechnol* **2009**, *19*, 1333-1341.

(11) Ornelas-Paz Jde, J.; Yahia, E. M.; Gardea-Bejar, A. *J Agric Food Chem* **2007**, *55*, 6628-6635.

(12) Aparicio-Ruiz, R.; Riedl, K. M.; Schwartz, S. J. *J Agric Food Chem* **2011**, *59*, 11100-11108.

(13) Gentili, A.; Caretti, F. *J Chromatogr A* **2011**, *1218*, 684-697.

(14) Garcia-de Blas, E.; Mateo, R.; Vinuela, J.; Alonso-Alvarez, C. *J Chromatogr B Analyt Technol Biomed Life Sci* **2011**, *879*, 341-348.

(15) Gauthier-Jaques, A.; Bortlik, K.; Hau, J.; Fay, L. B. *J Agric Food Chem* **2001**, *49*, 1117-1122.

(16) Rivera, S. M.; Canela-Garayoa, R. *J Chromatogr A* **2012**, *1224*, 1-10.

(17) Rivera, S. M.; Christou, P.; Canela-Garayoa, R. *Mass Spectrom Rev* **2013**.

(18) Liu, G. N.; Zhu, Y. H.; Jiang, J. G. *Appl Microbiol Biotechnol* **2009**, *83*, 989-999.

(19) Fu, W.; Paglia, G.; Magnusdottir, M.; Steinarsdottir, E. A.; Gudmundsson, S.; Palsson, B. O.; Andresson, O. S.; Brynjolfsson, S. *Microb Cell Fact* **2014**, *13*, 3.

(20) Hall, R. B., M.; Fiehn, O.; Hardy, N.; Sumner, L.; Bino, R. *Plant Cell* **2002**, *14*, 1437-1440.

(21) Paglia, G.; Williams, J. P.; Menikarachchi, L.; Thompson, J. W.; Tyldesley-Worster, R.; Halldorsson, S.; Rolfsson, O.; Moseley, A.; Grant, D.; Langridge, J.; Palsson, B. O.; Astarita, G. *Anal Chem* **2014**, *86*, 3985-3993.

(22) Kliman, M.; May, J. C.; McLean, J. A. *Biochim Biophys Acta* **2011**, *1811*, 935-945.

(23) Paglia, G.; Angel, P.; Williams, J. P.; Richardson, K.; Olivos, H. J.; Thompson, J. W.; Menikarachchi, L.; Lai, S.; Walsh, C.; Moseley, A.; Plumb, R. S.; Grant, D. F.; Palsson, B. O.; Langridge, J.; Geromanos, S.; Astarita, G. *Anal Chem* **2014**, *Accepted*.

(24) Zhang, L.; Foreman, D. P.; Grant, P. A.; Shrestha, B.; Moody, S. A.; Villiers, F.; Kwak, J. M.; Vertes, A. *Analyst* **2014**, *139*, 5079-5085.

(25) Stopka, S. A.; Shrestha, B.; Marechal, E.; Falconet, D.; Vertes, A. *Analyst* **2014**, *139*, 5945-5953.

(26) Stark, T. D.; Angelov, A.; Hofmann, M.; Liebl, W.; Hofmann, T. *Anal Bioanal Chem* **2013**, *405*, 9843-9848.

(27) Shah, V.; Castro-Perez, J. M.; McLaren, D. G.; Herath, K. B.; Previs, S. F.; Roddy, T. P. *Rapid Commun Mass Spectrom* **2013**, *27*, 2195-2200.

(28) Hart, P. J.; Francese, S.; Claude, E.; Woodroofe, M. N.; Clench, M. R. *Anal Bioanal Chem* **2011**, *401*, 115-125.

(29) Gonzales, G. B.; Raes, K.; Coelus, S.; Struijs, K.; Smagghe, G.; Van Camp, J. *J Chromatogr A* **2014**, *1323*, 39-48.

(30) Garmón-Lobato, S. A.-G., B.; Sánchez-Ilárduya, M.B.; Romera-Fernández, M.; Berrueta, L.A.; Gallo, B.; Vicente, F. *Anal Chim Acta* **2010**.

(31) Castro-Perez, J.; Roddy, T. P.; Nibbering, N. M.; Shah, V.; McLaren, D. G.; Previs, S.; Attygalle, A. B.; Herath, K.; Chen, Z.; Wang, S. P.; Mitnaul, L.; Hubbard, B. K.; Vreeken, R. J.; Johns, D. G.; Hankemeier, T. *J Am Soc Mass Spectrom* **2011**, *22*, 1552-1567.

(32) Dong, L.; Shion, H.; Davis, R. G.; Terry-Penak, B.; Castro-Perez, J.; van Breemen, R. B. *Anal Chem* **2010**.

(33) Bush, M. F.; Hall, Z.; Giles, K.; Hoyes, J.; Robinson, C. V.; Ruotolo, B. T. *Anal Chem* **2010**, *82*, 9557-9565.

(34) Bush, M. F.; Campuzano, I. D.; Robinson, C. V. *Anal Chem* **2012**, *84*, 7124-7130.

(35) Williams, J. P.; Lough, J. A.; Campuzano, I.; Richardson, K.; Sadler, P. J. *Rapid Commun Mass Spectrom* **2009**, *23*, 3563-3569.

(36) Fu, W.; Gudmundsson, O.; Feist, A. M.; Herjolfsson, G.; Brynjolfsson, S.; Palsson, B. O. *J Biotechnol* **2012**, *161*, 242-249.

(37) Fu, W.; Guethmundsson, O.; Paglia, G.; Herjolfsson, G.; Andresson, O. S.; Palsson, B. O.; Brynjolfsson, S. *Appl Microbiol Biotechnol* **2013**, *97*, 2395-2403.

(38) Garcia-Gonzalez, M.; Moreno, J.; Manzano, J. C.; Florencio, F. J.; Guerrero, M. G. *J Biotechnol* **2005**, *115*, 81-90.

(39) Fu, W.; Magnusdottir, M.; Brynjolfson, S.; Palsson, B. O.; Paglia, G. *Anal Bioanal Chem* **2012**, *404*, 3145-3154.

(40) Smith, C. A.; O'Maille, G.; Want, E. J.; Qin, C.; Trauger, S. A.; Brandon, T. R.; Custodio, D. E.; Abagyan, R.; Siuzdak, G. *Ther Drug Monit* **2005**, *27*, 747-751.

(41) Zhu, Z. J.; Schultz, A. W.; Wang, J.; Johnson, C. H.; Yannone, S. M.; Patti, G. J.; Siuzdak, G. *Nat Protoc* **2013**, *8*, 451-460.

(42) Fahy, E.; Subramaniam, S.; Murphy, R. C.; Nishijima, M.; Raetz, C. R.; Shimizu, T.; Spener, F.; van Meer, G.; Wakelam, M. J.; Dennis, E. A. *J Lipid Res* **2009**, *50 Suppl*, S9-14.

(43) Xia, J.; Mandal, R.; Sinelnikov, I. V.; Broadhurst, D.; Wishart, D. S. *Nucleic Acids Res* **2012**, *40*, W127-133.

(44) Evans, A. M. M., M.V.; Dai, H.; DeHaven, C.D. *Metabolomics: Open Access* **2012**, *2*, 110.

(45) Paglia, G.; Menikarachchi, L.; Langridge, J.; Astarita, G. In *Identification and Data Processing Methods in Metabolomics*; Rudaz, S., Ed.; Future Medicine: London, UK, 2014; Vol. In Press.

(46) Malkar, A. D., N.A.; Martin, H.J.; Patel, P.; Turner, M.A.; Watson, P.; Maughan, R.J.; Reid, H.J.; Sharp, B.L.; Thomas, C.L.P.; Reynolds, J.C.; Creaser, C.S. *Metabolomics* **2013**, *9*, 1192-1201.

(47) Dwivedi, P.; Schultz, A. J.; Hill, H. H. *Int J Mass Spectrom* **2010**, *298*, 78-90.

(48) Dwivedi, P.; Puzon, G.; Tam, M.; Langlais, D.; Jackson, S.; Kaplan, K.; Siems, W. F.; Schultz, A. J.; Xun, L.; Woods, A.; Hill, H. H., Jr. *J Mass Spectrom* **2010**, *45*, 1383-1393.

(49) Wichuk, K.; Brynjolfsson, S.; Fu, W. *Bioengineered* **2014**, *5*, 204-208.

Table 1. Tentative identifications of pigments using UHPLC-UV-TWIM-MS^E

Pigment	Metabolite	Formula	Adduct	Measured *m/z*	Theoretical *m/z*	Δppm	RT (min)	CCS (Å^2)
Carotene	β-carotene isomer I	C40H56	$[M]^+$	536.4351	536.4377	-4.8	16.80	**314**
Carotene	β-carotene Isomer II	C40H56	$[M]^+$	536.4350	536.4377	-5.0	16.97	**222**
Carotene	β-carotene	C40H56	$[M]^+$	536.4352	536.4377	-4.6	16.97	**316**
Xanthophyll	Cryptoxanthin isomer II	C40H56O	$[M]^+$	552.4380	552.4325	10.0	12.98	**321**
Xanthophyll	Cryptoxanthin isomer I	C40H56O	$[M]^+$	552.4336	552.4325	1.9	13.16	**320**
Xanthophyll	Zeaxanthin	C40H56O2	$[M]^+$	568.4320	568.4275	7.9	9.27	**266**
Xanthophyll	Lutein isomer II	C40H56O2	$[M]^+$	568.4223	568.4275	-9.2	9.37	**257**
Xanthophyll	Lutein	C40H56O2	$[M]^+$	568.4268	568.4275	-1.3	9.37	**325**
Xanthophyll	Lutein isomer I	C40H56O2	$[M]^+$	568.4310	568.4275	6.1	10.09	**319**
Xanthophyll	Diadinoxanthin isomer I	C40H54O3	$[M+H]^+$	583.4164	583.4157	1.1	7.87	**336**
Xanthophyll	Diadinoxanthin isomer II	C40H54O3	$[M+H]^+$	583.4121	583.4157	-6.2	8.88	**249**
Xanthophyll	Diadinoxanthin isomer III	C40H54O3	$[M+H]^+$	583.4135	583.4157	-3.9	8.88	**332**
Xanthophyll	Diadinoxanthin isomer IV	C40H54O3	$[M+H]^+$	583.4116	583.4157	-7.0	8.97	**317**
Xanthophyll	Antheraxanthin	C40H56O3	$[M+H]^+$	585.4252	585.4302	-8.5	8.30	**334**
Xanthophyll	Neoxanthin isomer I	C40H56O4	$[M+H]^+$	601.4211	601.4251	-6.7	5.95	**336**
Xanthophyll	Neoxanthin isomer II	C40H56O4	$[M+H]^+$	601.4297	601.4251	7.7	8.17	**258**
Xanthophyll	Fucoxanthin isomer I	C42H58O6	$[M+H]^+$	659.4312	659.4317	-0.7	6.36	**357**
Xanthophyll	Fucoxanthin isomer II	C42H58O6	$[M+H]^+$	659.4383	659.4317	9.9	6.36	**301**
Xanthophyll	Fucoxanthin isomer III	C42H58O6	$[M+H]^+$	659.4382	659.4317	9.8	6.36	**279**
Chlorophyll	Pheophytin a derivative	C55H72N4O5	$[M+H]^+$	869.5615	869.5575	4.6	15.37	**322**
Chlorophyll	Pheophytin a	C55H74N4O5	$[M+H]^+$	871.5743	871.5732	1.3	16.07	**326**
Chlorophyll	Pheophytin a'	C55H74N4O5	$[M+H]^+$	871.5771	871.5732	4.4	16.59	**324**
Chlorophyll	Pheophytin b	C55H72N4O6	$[M+H]^+$	885.5580	885.5525	6.2	14.40	**328**
Chlorophyll	Chlorophyll a derivative I	C55H68MgN4O5	$[M+H]^+$	889.5100	889.5113	-1.5	12.50	**326**
Chlorophyll	Chlorophyll a derivative	C55H70MgN4O5	$[M+H]^+$	891.5300	891.5269	3.5	13.00	**328**
Chlorophyll	Chlorophyll a' derivative	C55H70MgN4O5	$[M+H]^+$	891.5304	891.5269	3.9	13.30	**326**
Chlorophyll	Chlorophyll a	C55H72MgN4O5	$[M+H]^+$	893.5460	893.5426	3.8	13.51	**331**
Chlorophyll	Chlorophyll a'	C55H72MgN4O5	$[M+H]^+$	893.5468	893.5426	4.7	13.91	**328**
Chlorophyll	Chlorophyll b	C55H70MgN4O6	$[M+H]^+$	907.5284	907.5218	7.3	12.58	**331**
Chlorophyll	Chlorophyll b'	C55H70MgN4O6	$[M+H]^+$	907.5265	907.5218	5.2	12.95	**326**
Chlorophyll	Hydroxychlorophyll a	C55H72MgN4O6	$[M+H]^+$	909.5421	909.5375	5.0	13.18	**331**

Figure 1. Spectrophotometric filter for UPLC-TWIM-MS^E data. UHPLC-UV-TWIM-MS^E analysis of algae samples provided 6952 ion features (Raw data), each one characterized by *m/z*, retention time and CCS value. Features absorbing at 450 nm can be selectively extracted by aligning TWIM-MS and UV retention times.

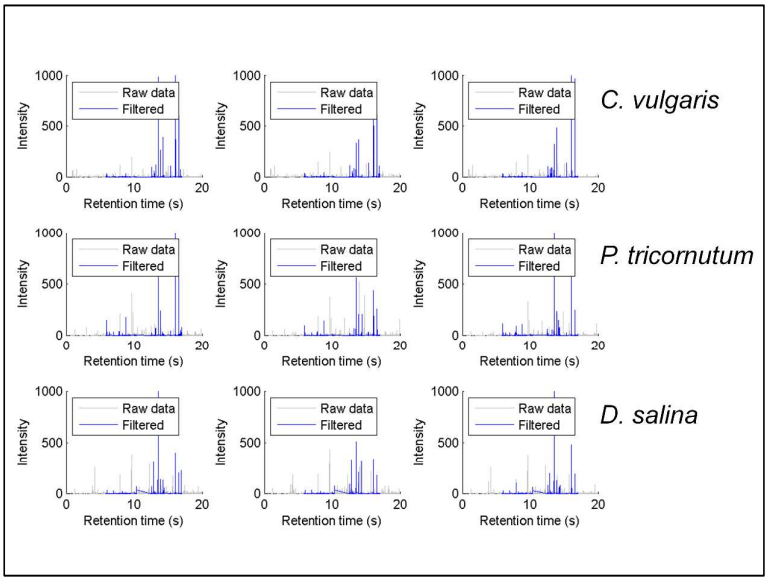

Figure 2. Isolating pigment features from raw complex UHPLC-UV-TWIM-MS data obtained from *C. vulgaris*. Retention time information for pigments absorbing at 450 nm was used as filter to isolate chlorophylls, xanthopylls and carotenes. Accurate mass measurement was combined with ion mobility information providing increased peak capacity and specificity, and resulting in separation of potential isomeric species.

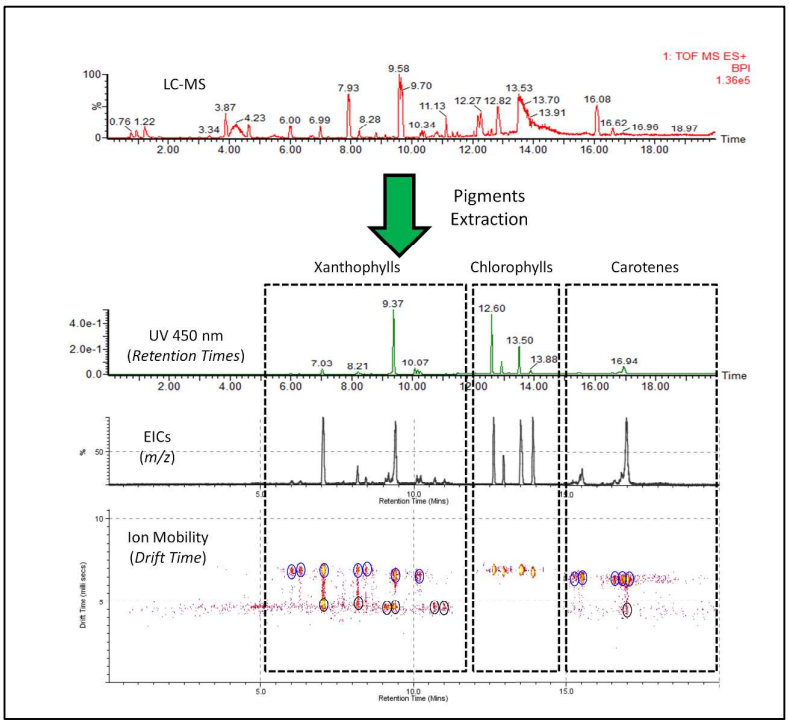

Figure 3. Identification of fucoxanthin isomers in *P. tricornutum*.

UHPLC-TWIM-MS^E allowed separating co-eluting isobaric species and simultaneously acquiring their fragmentation information in a single analytical run. The most abundant product ion resulting from the fragmentation of the precursor ion at *m/z* 659 was at *m/z* 641, resulting from the loss of water. The simultaneous loss of water and acetic acid from fucoxanthin generates the peak at *m/z* 581, which was detected from both isomer 1 and 2, but not from the isomer 3. Finally, the peak at *m/z* 109, visible only in the isomer 1, is likely due to the opening of the six-membered epoxide, together with the loss of water from the same ring, and the consequent formation of a carbonyl group in position to the ether.

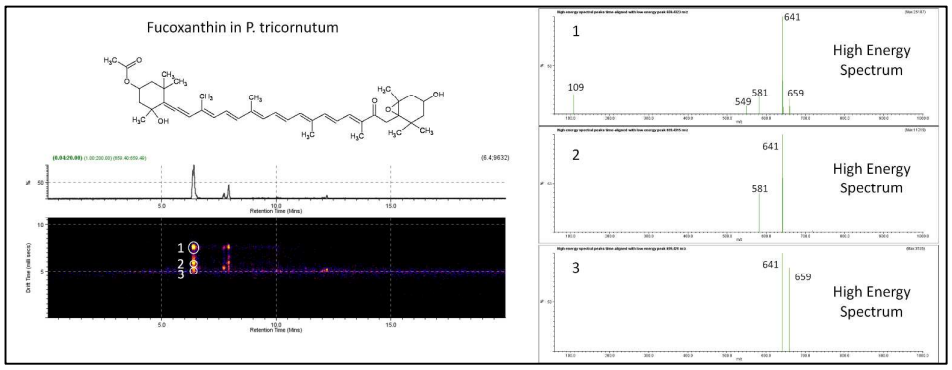

Figure 4. Phenotypic differentiation of microalgal species. a) Principal component analysis (PCA) provided clustering of the samples based on pigment composition, discriminating the three algae species. b) Hierarchical clustering analysis (HCA) showed a defined content of pigments for each algal species.

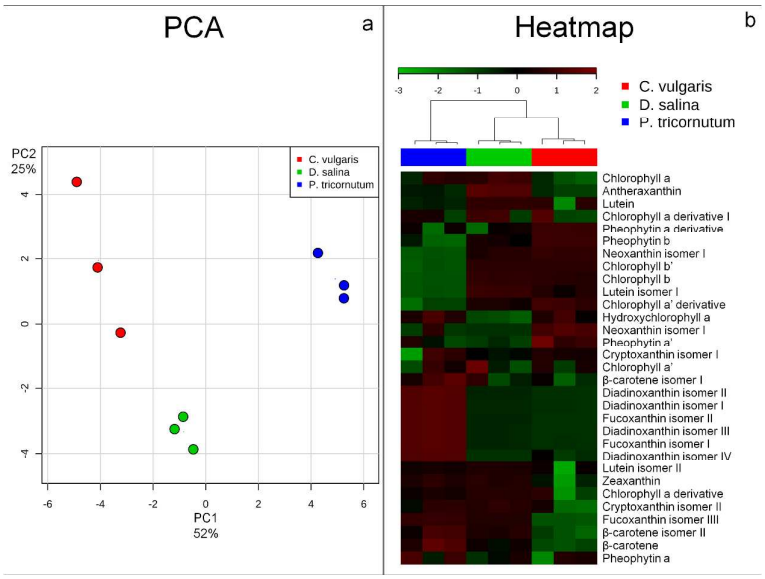

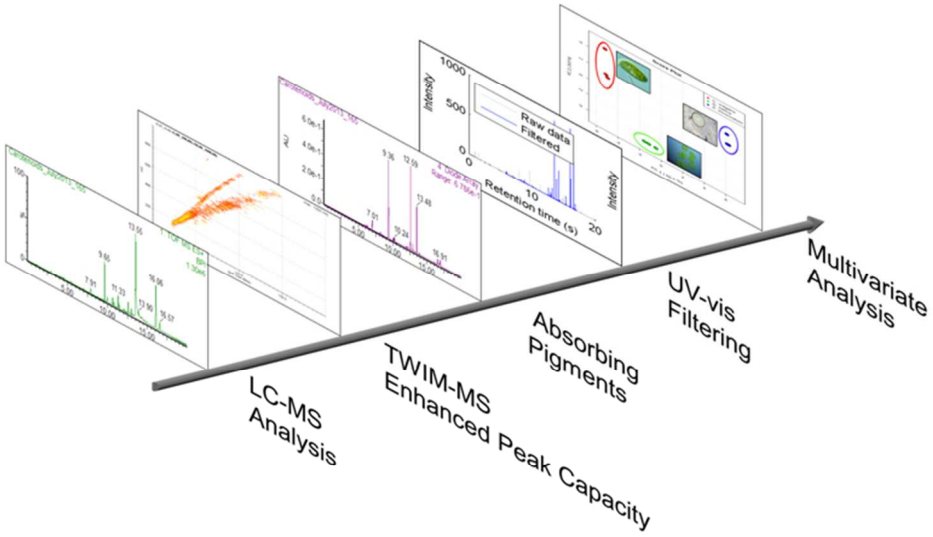

TOC Graphic
70x40mm (300 x 300 DPI)